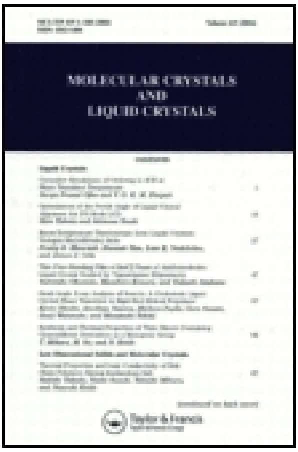

Molecular Crystals and Liquid Crystals
Publication details, including instructions for authors and subscription information:
http://www.tandfonline.com/loi/gmcl20

Liquid Crystal Structures for Transformation Optics

Jie Xiang [a] & Oleg D. Lavrentovich [a]
[a] Liquid Crystal Institute and Chemical Physics Interdisciplinary Program, Kent State University, Kent, Ohio, 44242
Version of record first published: 11 May 2012.

To cite this article: Jie Xiang & Oleg D. Lavrentovich (2012): Liquid Crystal Structures for Transformation Optics, Molecular Crystals and Liquid Crystals, 559:1, 106-114

To link to this article: http://dx.doi.org/10.1080/15421406.2012.658692

Mol. Cryst. Liq. Cryst., Vol. 559: pp. 106–114, 2012

ISSN: 1542-1406 print/1563-5287 online
DOI: 10.1080/15421406.2012.658692

Liquid Crystal Structures for Transformation Optics

JIE XIANG AND OLEG D. LAVRENTOVICH*

Liquid Crystal Institute and Chemical Physics Interdisciplinary Program, Kent State University, Kent, Ohio, 44242

We describe liquid crystal metamaterials (LCMMs), representing a composite of a uniaxial nematic liquid crystal as a dispersion medium and solid (metal) nanorods as a dispersed component. The purpose of the metal component is to vary the effective refractive indices and the resulting birefringence. By spatially distorting the optic axis of LCMMs or controlling concentration of the metallic component, one can design different trajectories of light as illustrated analytically for cylindrical samples of LCMMs.

Keywords Liquid crystal; metamaterial; nano-rods; transformation optics

1. Introduction

Transformation optics (TO) uses the equivalence of coordinate transformation and renormalization of material parameters (permittivity and permeability) to design a medium that controls propagation of light [1,2]. TO offers a wide range of potential applications, such as sub-wavelength imaging and focusing, invisibility cloaking, light trapping. Typically, the desired set of parameters is not naturally available and the corresponding material (called metamaterial) needs to be engineered from elements smaller than the wavelength λ of light but are assembled into structures much larger than λ. Fabrication at subwavelength scale by standard techniques such as lithography is challenging. Gradient distribution of the metamaterial properties is even more difficult. It is clear that development should include self-assembly. Self-assembled and reconfigurable metamaterials can be constructed in a variety of ways, for example, by dispersing and aligning gold nanorods (Au NRs) in lyotropic liquid crystals (LCs) [3], by creating Langmuir monolayers with nanoparticles at air-water interface [4,5], by heating and stretching nanoparticle/polymer composite films [6], or by condensing the isotropic dispersions of NRs into orientationally ordered arrays by dielectrophoretic effect [7,8]. A reversible assembly of Au NRs side-by-side or end-to-end with the help of chromonic aggregates have been demonstrated by Park et al. [9] Several groups explore LCs as filler material for nanostructures with plasmonic response. For example, Smalley et al. demonstrated a high contrast nanoplasmonic modulator with a dual-frequency LC [10], while Zhang et al. varied the refractive index of fishnet nanostructured metamaterial with an embedded nematic LC [11].

It is clear that both the assembly and performance of metamaterials might greatly benefit from having a liquid crystal (LC) as part of the structure [12]. LCs are known for their role in displays, made possible by significant optical birefringence $\Delta n = n_e - n_o$:

*Address correspondence to Oleg D. Lavrentovich, Liquid Crystal Institute and Chemical Physics Interdisciplinary Program, Kent State University, Kent, Ohio, 44242. Phone: 1 330 672-4844; Fax: 1 330 672-2796. E-mail: olavrent@kent.edu

for the typical LC mixture E7 (Merck), the ordinary refractive index n_o is 1.52, while the extraordinary index n_e is 1.74 at $\lambda = 700$ nm. For comparison, in calcite, a uniaxial solid birefringent crystal, $n_o = 1.49$ and $n_e = 1.66$ at 590 nm [13]. Lately, solid birefringent dielectrics attracted a renewed interest from the point of view of optical manipulation such as invisibility cloaking [13] and control of rays trajectories [14]. An obvious advantage of LCs in the construction of devices that control light propagation is that the local optic axis (the director $\hat{\boldsymbol{n}}$) can be made varying in space and time. A certain drawback of LCs is that director fluctuations cause light scattering which becomes stronger as birefringence increases; the effect might preclude the usage of thick LC cells. However, light scattering caused by director fluctuations can be mitigated, for example, when well-aligned smectic materials are used instead of nematic LCs.

The concepts of TO are not entirely new to the science of LCs. In 1919, Grandjean [15] considered a cylindrical nematic sample in which the director $\hat{n}$ was arranged radially. When such a structure is illuminated with light polarized normally to the cylinder, the rays are bent away from the central axis and leave a segment of an opening angle $2\pi(1 - n_o/n_e)$ unilluminated (for a modern reproduction of the result, see the textbook [16]). This particular example represents a beam divider, as the trajectories are splitting into different pathways. This pioneering work of Grandjean has recently been substantially expanded by Sátiro and Moraes [17,18] who considered other types of director configurations, such as disclinations of strength "1/2" and "$-1/2$". Light propagation was analyzed as a function of temperature- and wavelength-dependent refractive indices n_e and n_o [18].

In this work, we extend the consideration of curved light trajectories from a standard LC to a "LC metamaterial", or LCMM, i.e. a material representing a dispersion of a solid (metallic) component such as Au NRs in a uniaxial nematic LC as a dispersion matrix. The LC matrix aligns the NRs along $\hat{\boldsymbol{n}}$. The NRs are much smaller than λ so that the composite is optically homogeneous. Recent experiments with NRs assembled into orientationally ordered substrutures, see, for example, ref. [19] and the works mentioned above, suggest that construction of LCMMs is feasible. The optical properties of LCMM can be potentially controlled at three different levels. At the first level, by controlling the shape and concentration of solid inclusions, one can control the refractive indices. Typically, the metallic component decreases the effective refractive index (and increases light absorption). At the second level, with a given composition and concentration of the components, one can reconfigure and switch the optic axis. Finally, at the third level, the distortions of optics axis can be supplemented by gradients of the composition. For example, as shown by Golovin et al. [7,8], application of a gradient electric field to an isotropic dispersion of Au NRs results in the condensation of Au NRs into orientationally ordered structures with spatially-varying concentration, birefringence and optical axis.

In this work, we consider LCMM properties controlled at the level 1 and 2, i.e., with birefringence set up by the concentration of metal NRs dispersed in a thermotropic nematic LC and the configuration of optical axis controlled by the boundary conditions in a sample shaped as a cylindrical shell. We describe analytically light refraction at the isotropic-LCMM interface and light propagation for the case when the director, the wave-vector and the direction of linear polarization of light are confined to the same (x, y) plane.

2. Refractive Indices of LCMM

The LCMMs in this work represents a dispersion of rod-like metallic particles, say, Au NRs, in an uniaxial nematic LC. Concentration of the metallic part that is constant throughout

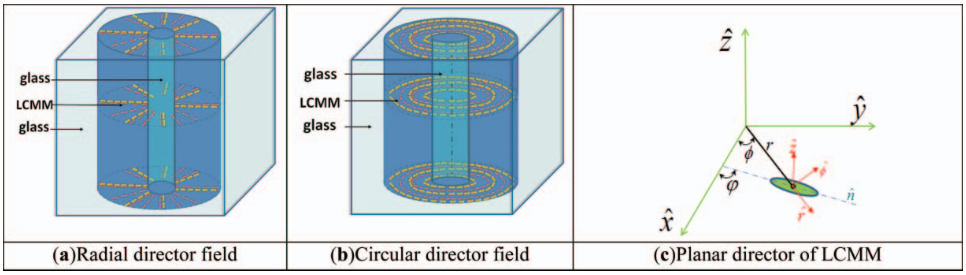

Figure 1. Director configurations for LCMM in a cylindrical shell, $a \leq r \leq b$, with the optic axis represented in the cylindrical coordinates (r, φ, z) as (a) $\hat{n} = (1, 0, 0)$; (b) $\hat{n} = (0, 1, 0)$; (c) planar director orientation in the Cartesian and cylindrical coordinates.

the sample controls the dielectric properties. We consider two director configurations in a cylindrical LCMM shell stabilized by the surface anchoring, Figs 1(a) and (b).

For a composite medium with two anisotropic uniaxial components, namely, the metal NRs and LC, with the same director, the effective optical properties can be described by the model of Sihvola [20]. Suppose that each NR is a spheroid with semi-axes a_x, a_y and $a_z (a_x > a_y = a_z)$ and (isotropic) dielectric permittivity ε_m. The NRs are embedded into the LC characterized by a permittivity tensor $\bar{\bar{\varepsilon}}_{LC}$. We neglect the optical properties of the thin functionalizing layers at the surface of NRs that prevent aggregation of the NRs. Then the effective permittivity tensor of the LCMM is

$$\bar{\bar{\varepsilon}}_{LCMM} = \bar{\bar{\varepsilon}}_{LC} + \frac{f(\varepsilon_m \cdot \bar{\bar{I}} - \bar{\bar{\varepsilon}}_{LC}) \cdot \bar{\bar{\varepsilon}}_{LC}}{\bar{\bar{\varepsilon}}_{LC} + (1-f) \cdot \bar{\bar{L}} \cdot (\varepsilon_m \cdot \bar{\bar{I}} - \bar{\bar{\varepsilon}}_{LC})}, \quad (1)$$

where $\bar{\bar{I}}$ is the identity matrix, f and *1-f* are the volume fractions of the NRs and LC, respectively, and $\bar{\bar{L}}$ is the transformed depolarization dyadic,

$$\bar{\bar{L}} = \frac{\det \bar{\bar{A}}}{2} \int_0^\infty \frac{\bar{\bar{\varepsilon}}_{LC} \cdot ds}{(\bar{\bar{A}}^2 + \bar{\bar{\varepsilon}}_{LC} \cdot s)\sqrt{\det(\bar{\bar{A}}^2 + \bar{\bar{\varepsilon}}_{LC} \cdot s)}}; \quad (2)$$

Furthermore, $\bar{\bar{A}} = \left[\begin{matrix} a_x & 0 & 0 \\ 0 & a_y & 0 \\ 0 & 0 & a_z \end{matrix} \right]$ and $\det \bar{\bar{A}} = a_x a_y a_z$. With the given ε_m, $\bar{\bar{\varepsilon}}_{LC}$, a_x and a_y, $\bar{\bar{\varepsilon}}_{LCMM}$ can be controlled by changing the volume fraction of NRs. To describe the effective refractive indices of the LCMM we use the same notations n_e and n_o as in the case of the regular LCs; the presence of NRs in LC changes only the values of the refractive indices but does not change the general uniaxial non-polar symmetry of the medium.

Consider, for example, an LCMM comprised of a LC E7 with $n_o = 1.52$ and $n_e = 1.74$, doped with Au NRs of $a_x = 60$ nm and $a_y = a_z = 15$ nm. For Au, $\varepsilon_m = -16.7$ at 700 nm [21]. The effective extraordinary refractive index n_e of LCMM calculated according to equation (1), decreases sharply as a function of *f*, first becoming equal to n_o at $f = 0.013$, and then turning zero at a relatively modest *f* just above 0.07, Fig. 2.

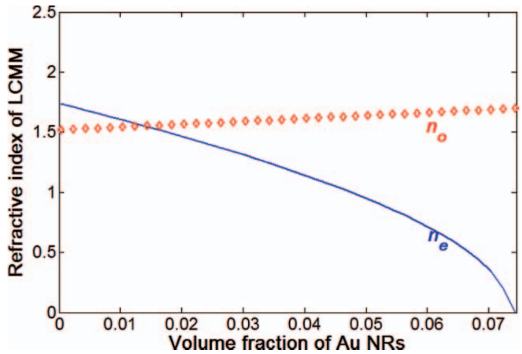

Figure 2. Effective refractive indices (n_e, n_o) of LCMM, which is composed of a LC matrix E7 with $n_o = 1.52$ and $n_e = 1.74$ doped with Au NRs of $a_x = 60$ nm and $a_y = a_z = 15$ nm.

3. Light Propagation in Distorted Planar LCMM

In this section, we consider planar director field $\hat{\boldsymbol{n}} = (n_x, n_y, 0)$; the wave-vector and polarization of light are also confined to the same (x, y) plane. We first discuss light refraction at the LCMM-isotropic interface. The results will be used later to describe light propagation through a cylindrical LCMM shell with an isotropic medium inside and outside.

3.1 Refraction at the Interface Between Isotropic and Anisotropic Medium

Refraction at an interface of two different isotropic media is described by the Snell's law, that is based on the condition that the tangential components of wavevectors on the two sides of the interface are equal to each other [22]. The time averaged Poynting vector for the transmitted light, which defines the actual direction of the energy flow of the light, has the same direction as the transmitted wavevector. When light with an angle of incidence θ_i experiences refraction at the interface between an isotropic and an anisotropic medium, the directions of wave vector $\boldsymbol{k}_t$ and Poynting vector $\boldsymbol{S}_t$ for the transmitted light would be generally different, $\theta_{t,k} \neq \theta_{t,S}$, Fig. 3.

As shown in refs. [23,24], if the uniaxial medium has the optic axis tilted by an angle α with respect to the interface, and an incident plane wave is linearly polarized in the xy plane, these two angles, measured with respect to the x-axis (normal to the interface) in Fig. 3, write

$$\theta_{t,k} = \tan^{-1}\left(\frac{2bn_i \sin\theta_i}{\sqrt{\left(c^2 - 4ab\right) n_i^2 \sin^2\theta_i + 4b} - cn_i \sin\theta_i}\right); \quad (3)$$

$$\theta_{t,S} = \tan^{-1}\left(\frac{\left(4ab - c^2\right) n_i \sin\theta_i}{2b\sqrt{\left(c^2 - 4ab\right) n_i^2 \sin^2\theta_i + 4b}} + \frac{c}{2b}\right);$$

where $a = \frac{1}{n_e^2 n_o^2}(n_o^2 \sin^2\alpha + n_e^2 \cos^2\alpha)$, $b = \frac{1}{n_e^2 n_o^2}(n_o^2 \cos^2\alpha + n_e^2 \sin^2\alpha)$, $c = \frac{1}{n_e^2 n_o^2}(n_o - n_e)$ $\sin(2\alpha)$.

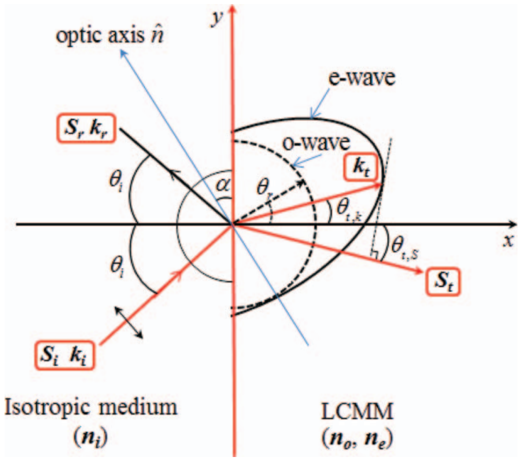

Figure 3. Refraction at the isotropic-anisotropic media interface. The incident beam is polarized in the plane of the figure. The wave vector surfaces are shown as a solid circle for isotropic medium, as a solid ellipse for the extraordinary wave, and as a dashed circle for the ordinary wave in the anisotropic medium.

The reflection coefficient in this case can be written in the form [25]

$$r = \frac{n_i\sqrt{n_r^2 - n_i^2 \sin^2\theta_i} - n_e n_o \cos\theta_i}{n_i\sqrt{n_r^2 - n_i^2 \sin^2\theta_i} + n_e n_o \cos\theta_i} \tag{4}$$

where $n_r = \sqrt{n_o^2 + (n_e^2 - n_o^2)\sin^2\alpha}$. Total reflection happens when $|r| = 1$. Equation (3) will be used to calculate refraction at the outer and inner surfaces of the LCMM shell. In some cases, such as a planar director field within the shell, the trajectories can be found analytically; this case is treated below.

3.2 Light Propagation Through the LCMM Bulk with Planar Director

Propagation of light in an isotropic medium is described by Fermat's principle, stating that the trajectory of light between two points corresponds to a minimum of time spent to travel. The time of travel is determined by the product of the physical length and the refractive index [26] which might vary in space. To describe an anisotropic medium, we follow Joets and Ribotta [27] and Sátiro and Moraes [17,18], who interpreted the Fermat's principle through geodesics in Finsler geometry. The Finsler geometry considers a line element of the trajectory as being dependent not only on the location but also on the orientation,

$$ds = F(x, \dot{x})\, dt, \tag{5}$$

where $F(x, \dot{x})$ is the Finslerian function, x and $\dot{x} = dx/dt$ are the space coordinates and its derivative with respect to the line element parameter t, respectively. In geometric optics for anisotropic medium, Finslerian function reads

$$F(x, \dot{x}) = N_r \cdot \|\dot{x}\| \tag{6}$$

where $|\dot{x}| = \sqrt{\dot{x}^T \cdot \dot{x}}$ is the ordinary distance from the origin to the point $\dot{x}$ and $\dot{x}^T$ is the transpose of vector $\dot{x}$. $N_r = \sqrt{n_o^2 \cos^2\beta + n_e^2 \sin^2\beta}$ is the refractive index for the

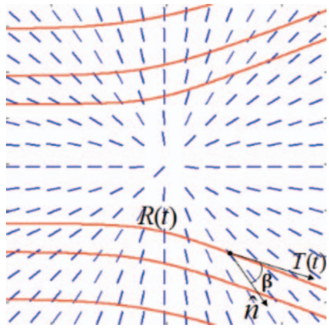

Figure 4. Illustration of the light path $\mathbf{R}(t)$in planar radial director field, its tangential vector $T(t)$ and the director $\hat{n}$ of LCMM.

extraordinary ray, associated with the energy velocity, and β is the local angle made by wave vector and Poynting vector.

As already stressed, in this section we study LCMM with a planar director; the wavevector and polarization of light are confined to the same plane. The spatially-varying director has the components $\hat{\boldsymbol{n}} = (\cos\varphi,\ \sin\varphi,\ 0)$ in Cartesian coordinates, where φ is the angle between the director and x-axis in Cartesian coordinates, $\varphi = k\phi + c$; k and c are constants; ϕ is an azimuthal angle between the r-axis in cylindrical coordinates and x-axis in Cartesian coordinates, Fig. 1(c). For the planar radial director field, $k = 1$ and $c = 0$, Fig. 1(a). For the planar circular director field, $k = 1$ and $c = \pi/2$, Fig. 1(b). The light trajectory is written as [15] $\boldsymbol{R}(t) = r(t)\cos\phi(t)\hat{x} + r(t)\sin\phi(t)\hat{y}$, Fig. 4, combining the cylindrical coordinates r and ϕ with the Cartesian basis $\{\hat{x}, \hat{y}\}$. Then $\boldsymbol{T}(t) = d\boldsymbol{R}/dt$ is the tangential vector to the light path at each position parameterized by t; the angle β is calculated from the formula $\cos\beta = \boldsymbol{T} \cdot \hat{\boldsymbol{n}}/||\boldsymbol{T}||$. The path of light ray minimizes the "distance" $\int ds$, which leads to an interpretation of the light paths as a geodesic in the Finsler space [17,18,27,28],

$$\frac{d^2x^i}{dt^2} + \sum_{j,k} \Gamma^i_{jk} \frac{dx^j}{dt}\frac{dx^k}{dt} = 0 \tag{7}$$

where t is the ray parameter along the geodesic and Γ^i_{jk} are Christoffel symbols; i, j and k are the indices representing different components of the spatial coordinates x.

In the cases of planar radial director field, the geodesic equations (7) transform into the coupled ordinary differential equations in the cylindrical coordinates [18]

$$\begin{aligned} \frac{d^2r}{dt^2} - \gamma^2 r\left(\frac{d\phi}{dt}\right)^2 &= 0 \\ \frac{d^2\phi}{dt^2} - \frac{2}{r}\frac{dr}{dt}\frac{d\phi}{dt} &= 0 \end{aligned} \tag{8}$$

with the solutions

$$\begin{aligned} r(t) &= \sqrt{\frac{C^2}{2E\gamma^2} + 2E\,(t+D)^2} \\ \phi(t) &= \frac{1}{\gamma}\arctan\left(\frac{2E\gamma\,(t+D)}{C}\right) + F \end{aligned} \tag{9}$$

where C, D, E and $F$are integration constants, which can be obtained by the boundary condition, such as the position and direction of the incident light ray, and $\gamma = n_e/n_o$. The expressions are the same as those derived by Sátiro and Moraes [18] with the difference that the first term in the expression for $r(t)$ is written as $C^2/E\gamma^2$ in ref. [18] and our calculations show this term as $C^2/2E\gamma^2$. For the circular director field, the solutions for light trajectories are the same as in equation (9), with that difference that $\gamma = n_o/n_e$.

3.3 Light Trajectory through a Cylindrical Shell with Planar Director

Using the rules of refraction at the interface of isotropic-anisotropic media and light propagation in anisotropic medium as discussed above, we can find analytically the light trajectories for the structure shown in Fig. 1(b), a cylindrical shell filled with a LCMM that has a circular director configuration, stabilized by anchoring at the two bounding cylindrical surfaces. The inside and outside of the shell is filled with glass of a refractive index 1.52. For the pure LC (no added NRs), $n_e = 1.74$ and $n_o = 1.52$. A pure LC shell bends the light beams towards the center, Fig. 5(a). For example, for beam No.1 in Fig. 5(a), the incident angle θ_i is 0.785; the refraction angle is $\theta_{t,S} = 0.853$ as follows from equation (3); the integration constants(C, D, E, F) in equation (9) are calculated as (−5.852, −7.551, 0.439, 1.297). The beam propagates through the LCMM-glass interface following equation (9) and exits from the LCMM at the point (8.371, 5.470) under the angle (−0.785).

By adding NRs to the mixture, one effectively decreases n_e. For example, $n_e = 1.3$ if the LC is doped with the Au NRs (diameter 15 nm, length 60 nm) of volume fraction 0.041. The ordinary index n_o changes little because the response of a NR to the electric field oriented normal to the NR is weak, and at low volume fraction of Au NRs it can be neglected. Birefringence becomes negative and the incident light beams bend away from the center, Fig. 5(b). Further decrease of n_e to 0.8 (for the volume fraction of the Au NRs at 0.057) results in the appearance of two focus points at the outer surface of the shell, Fig. 5(c), which can be used in solar energy concentrators.

The director of LCMM can be reconfigured from a circular configuration to a radial and visa versa, say, by changing the surface anchoring direction. Figure 6 shows in-plane polarized light beams propagating in a LCMM shell with a radial director. As compared to Fig. 5, the results are completely different. For the pure LC with $n_e = 1.74$ and $n_o = 1.52$, the incident parallel light beams converge, Fig. 6(a). When n_e is reduced to 1.3 while n_o remains the same, the light beams diverge, Fig. 6(b). When $n_e = 0.8$, some of the incident

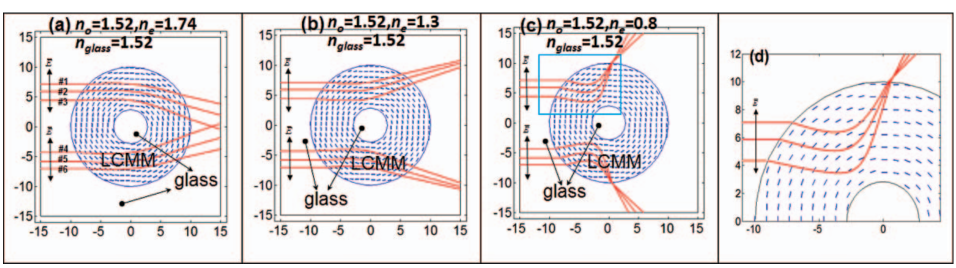

Figure 5. Light trajectories for LCMM cylindrical shell with circular director and different refractive indices: (a) $n_o = 1.52$, $n_e = 1.74$; (b) $n_o = 1.52$, $n_e = 1.3$; (c) $n_o = 1.52$, $n_e = 0.8$. (d) Magnified image of rectangular area in (c).

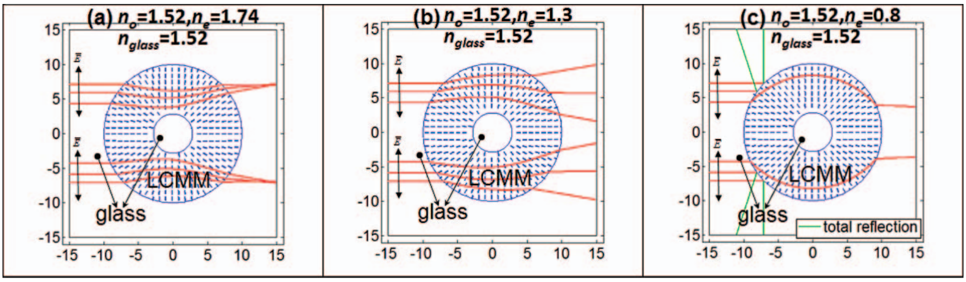

Figure 6. Light trajectories for LCMM cylindrical shell sample with radial director and different refractive indices: (a) $n_o = 1.52$, $n_e = 1.74$; (b) $n_o = 1.52$, $n_e = 1.3$; (c) $n_o = 1.52$, $n_e = 0.8$.

beams (those that are further away from the center) are totally reflected at the glass-LCMM interface, Fig. 6(c). Note that Fig. 5 and 6 do not show the beams partially reflected at the glass-LCMM interface.

4. Conclusion

We demonstrated that LCMMs, representing liquid crystal-metal nanorods compositions, in which small metallic nanorods are aligned by the LC matrix, can be used for the control of light propagation. For planar radial and circular geometries of the director field, the LCMM cylindrical shells can either converge or diverge the light beams polarized in the plane of the director. We considered only zero-pretilt surface anchoring in the cylindrical capillary structure. By using titled boundary conditions [24] and electric fields [29], one can create many other configurations of the director. By controlling also the local value of the metal filling factor, one can add another approach to the reconfigurable LCMMs. Note that in this work we did not consider a possible effect of director reorientation by the electric field of the propagating wave, which might occur at high intensities [30]. It would be of interest to supplement the consideration with strongly nonlinear effects such as formation of optical spatial solitons, called “nematicons” [31–33], that might also contribute to the controlling mechanisms of LCMMs.

Acknowledgments

This work was supported by AFOSR FA9550-10-1-0527 grant and NSF grant DMR 1121288.

References

[1] Schurig, D., Mock, J. J., Justice, B. J., Cummer, S. A., Pendry, J. B., Starr, A. F., & Smith, D. R. (2006). *Science*, *314*, 977–980.
[2] Cai, W., & Shalaev, V. M. (2010). *Optical Metamaterials: Fundamentals and Applications*, Springer: New York.
[3] Liu, Q. K., Cui, Y. X., Gardner, D., Li, X., He, S. L., & Smalyukh, I. I. (2010). *Nano Lett.*, *10*, 1347–1353.
[4] Fukuto, M., Heilmann, R. K., Pershan, P. S., Badia, A., & Lennox, R. B. (2004). *J. Chem. Phys.*, *120*, 3446–3459.
[5] Zhang, L., Shen, Y. H., Xie, A. J., Li, S. K., Jin, B. K., & Zhang, Q. F. (2006). *J. Phys. Chem. B*, *110*, 6615–6620.

[6] Perez-Juste, J., Rodriguez-Gonzalez, B., Mulvaney, P., & Liz-Marzan, L. M. (2005). *Adv. Funct. Mater.*, *15*, 1065–1071.
[7] Golovin, A. B., & Lavrentovich, O. D. (2009). *Appl. Phys. Lett.*, *95*, 254104.
[8] Golovin, A. B., Xiang, J., Park, H.-S., Tortora, L., Nastishin, Y. A., Shiyanovskii, S. V., & Lavrentovich, O. D. (2011). *Materials*, *4*, 390–416.
[9] Park, H. S., Agarwal, A., Kotov, N. A., & Lavrentovich, O. D. (2008). *Langmuir*, *24*, 13833–13837.
[10] Smalley, J. S. T., Zhao, Y. H., Nawaz, A. A., Hao, Q. Z., Ma, Y., Khoo, I. C., & Huang, T. J. (2011). *Opt. Express*, *19*, 15265–15274.
[11] Zhang, F. L., Zhang, W. H., Zhao, Q., Sun, J. B., Qiu, K. P., Zhou, J., & Lippens, D. (2011). *Opt. Express*, *19*, 1563–1568.
[12] Lavrentovich, O. D. (2011). *P Natl. Acad. Sci. USA*, *108*, 5143–5144.
[13] Zhang, S. A., Chen, X. Z., Luo, Y., Zhang, J. J., Jiang, K., & Pendry, J. B. (2011). *Nat. Commun.*, *2*, 176.
[14] Danner, A. J., Tyc, T., & Leonhardt, U. (2011). *Nat. Photonics*, *5*, 357–359.
[15] Grandjean, F. B. (1919). *Soc. Franc. Minèralogie*, *42*, 42–86.
[16] Kleman, M., & Lavrentovich, O. D. (2003). *Soft Matter Physics: An Introduction*, Springer: New York.
[17] Satiro, C., & Moraes, F. (2006). *Eur. Phys. J. E.*, *20*, 173–178.
[18] Satiro, C., & Moraes, F. (2008). *Eur. Phys. J. E.*, *25*, 425–429.
[19] Evans, J. S., Beier, C. N., & Smalyukh, I. I. (2011). *J. Appl. Phys.*, *110*, 033535.
[20] Sihvola, A. (1999). *Electromagnetic Mixing Formulas and Applications*, Institution of Electrical Engineers: London.
[21] Palik, E. D., & Ghosh, G. (1998). *Handbook of Optical Constants of Solids*, Academic Press: San Diego.
[22] Fowles, G. R. (1989). *Introduction to Modern Optics,* 2nd ed. Dover Publications: New York.
[23] Luo, H. L., Hu, W., Yi, X. N., Liu, H. Y., & Zhu, J. (2005). *Opt. Commun.*, *254*, 353–360.
[24] Pishnyak, O. P., & Lavrentovich, O. D. (2006). *Appl. Phys. Lett.*, *89*, 251103.
[25] Lekner, J. (1993). *J. Opt. Soc. Am. A.*, *10*, 2059–2064.
[26] Born, M., & Wolf, E. (1999). *Principles of Optics: Electromagnetic Theory of Propagation, Interference and Diffraction of Light,* 7th expanded ed. Cambridge University Press: Cambridge, New York.
[27] Joets, A., & Ribotta, R. (1994). *Opt. Commun.*, *107*, 200–204.
[28] Perlick, V. (2006). *Gen. Relat. Gravit.*, *38*, 365–380.
[29] Peccianti, M., Dyadyusha, A., Kaczmarek, M., & Assanto, G. (2006). *Nat. Phys.*, *2*, 737–742.
[30] Khoo, I.-C., & Wu, S.-T. (1993). *Optics and Nonlinear Optics of Liquid Crystals*, World Scientific: Singapore.
[31] Barboza, R., Alberucci, A., & Assanto, G. (2011). *Opt. Lett.*, *36*, 2725–2727.
[32] Izdebskaya, Y. V., Shvedov, V. G., Desyatnikov, A. S., Krolikowski, W., & Kivshar, Y. S. (2010). *Opt. Lett.*, *35*, 1692–1694.
[33] Peccianti, M., Assanto, G., Dyadyusha, A., & Kaczmarek, M. (2007). *Phys. Rev. Lett.*, *98*, 113902.